Polar-Reflection Faraday Effect and the Fermi Surface of α-Phase Silver-Magnesium and Silver-Cadmium Alloys*

J. M. Tracy† and E. A. Stern
Physics Department, University of Washington, Seattle, Washington 98195
(Received 13 November 1972)

The Fermi surfaces of α-phase disordered AgCd and AgMg alloys have been studied using the polar-reflection Faraday effect. Concentrations as high as 39.3-at.% Cd and 30.0-at.% Mg were obtained. It is shown that the uncertainty in the energy of states on the Fermi surface is small compared to changes which occur on alloying. Thus in both alloy systems, the Fermi surface is still a valid concept to use in discussing electronic properties of the concentrated alloys. It is found that the Fermi surfaces of both AgMg and AgCd change the same with concentration within experimental error up to 30 at.%, the maximum solubility of Mg in the α phase. The Fermi-surface necks continually increase in size faster than the belly dimensions with increasing Cd and Mg content. There is some evidence that the AgCd Fermi surface may have a second contact near 40-at.% Cd. By comparison with room-temperature Hall-effect measurements, it is determined that for concentrated alloys the ratio of the room-temperature relaxation time on the belly, τ_B, to that on the neck, τ_N, is $\tau_B/\tau_N = 1 \pm 0.2$ for both AgMg and AgCd. In spite of the similarities of the Fermi surfaces for both AgMg and AgCd, only AgCd satisfies the Hume-Rothery rules. This is the first experimental evidence that the simple explanation that the Hume-Rothery rules depend only on Fermi-surface properties of the α phase is inadequate.

I. INTRODUCTION

It is of interest to study the Fermi surface of concentrated alloys in order to understand what happens to the distribution of the conduction electrons when an impurity atom disrupts the periodic potential of the pure-metal lattice. There are two main points to consider: whether or not one can actually define a Fermi surface for concentrated alloys and, if so, how do its dimensions change when the impurity concentration is changed. Strictly speaking, an electron of given wave vector will not have a perfectly well-defined energy if there is even one impurity atom in the host. However, for sufficiently dilute impurities, the concept of a sharp Fermi surface works quite well because the uncertainty in the Fermi energy is negligible compared to its dimensions. For concentrated alloys this may no longer be the case, and ideas which depend on the geometry of the distribution of electrons in k space have to be modified.

To understand which view is appropriate for noble-metal alloys, it is essential to do experiments which measure the uncertainty or smearing of the Fermi surface as well as its dimensions. For pure metals there are some techniques which give highly accurate Fermi-surface dimensions and recently have been able to reveal information about Fermi-surface properties of dilute alloys. However, most of these techniques have limited use in concentrated alloys because of the condition that the average electron lifetime τ must be longer than the inverse of a comparatively low frequency such as the cyclotron frequency. Therefore they cannot be used for alloys with more than a small fraction of a percent impurity content. The polar-reflection Faraday effect (PRFE) avoids this difficulty and gives useful information about the Fermi surface provided $\tau \gg 1/\omega$, where ω is the frequency of light used. Since the angular frequency of 1-μm radiation is about 2×10^{-15} sec^{-1}, this condition may be satisfied in some alloys. It will be shown later that this last condition is just what is needed for the Fermi surface to be reasonably well defined.

The PRFE has been used previously[1,2] to investigate pure Ag, Al, Au, and AgAu alloys. The latter measurements showed that the Fermi-surface neck diameter increased monotonically from pure Ag to pure Au. We have extended the measurements of the α phase of AgMg and AgCd. In these alloys, the situation is quite different than in AgAu because Cd and Mg have two conduction electrons per atom. Therefore if the extra electrons go into conduction states, the number of states in the conduction band increases and the Fermi surface must expand to accomodate this. It is also expected that electron lifetimes will be shortened more than in the case of AgAu because of the increased potential difference between host and impurity. For the case of monovalent impurities there is no net charge to be screened, and the change in each wave function in the vicinity of an impurity site is small. This then implies that the smearing of the electron wave vector is small and the electron states may be described as approximate Bloch states. This has been shown experimentally.[2] With divalent impurities, the screening charge must be doubled around each impurity atom. This means there must be a large change in the wave function at the impurity site. How-

ever, this does not necessarily mean that the smearing of the Fermi surface is large. In fact, because of band-structure effects on the screening cloud surrounding impurities, one expects that the smearing of the Fermi surface due to alloying in the systems considered here should be small compared to changes in its size. This is demonstrated to be the case later in this paper. A more detailed discussion of these points is given in Ref. 3.

In Ref. 3 it is shown that the general condition that an alloy must satisfy in order that the description used above of a Fermi surface and its changes in dimension on alloying be valid for all concentrations is that $x^2 \equiv \Delta E_i / \Delta E_r \ll 1$. Here ΔE_r and ΔE_i are the real and imaginary parts of the energy shift of an average electron state at the Fermi surface induced by alloying. ΔE_i can be estimated by electrical-resistance measurements and ΔE_r can be estimated by a rigid-band model.[3] Estimates obtained in this manner for AgCd and AgMg are $x^2 \simeq 0.2$, and we expect that the Fermi surface will be reasonably well defined for all concentrations. The measurements to be described verify this prediction.

The choice of alloys to be studied was dictated by several considerations. Noble metals have been studied before with the PRFE and they have simple Fermi surfaces contained in one zone. Ag-based alloys were chosen because of the poor alloying behavior of Au and because Cu oxidizes in air. Furthermore, Cd and Mg impurities in Ag give rise to the smallest values of residual resistance of any polyvalent impurities and thus one expects the smallest values for x^2. Both cause similar expansion of the lattice; nevertheless, the α-phase boundaries for both alloys are quite different. The solubility of Cd in Ag is about 42 at.% while for Mg the figure is only about 30 at.%. AgCd is known as a Hume-Rothery alloy while AgMg is not.[4] So these are interesting choices on which to make Fermi surface measurements. Of course the stability of AgMg is affected by the fact that the stable higher-concentration phase is ordered, while this is not so for AgCd. A simple explanation of the Hume-Rothery rules in terms of the electronic density of states will not suffice, as will be discussed later in this paper. Comparison of Mg and Cd as solutes may be useful for another reason. It is known that the geometry of the Fermi surface in noble metals depends largely on properties of the d bands. Cd has d bands similar to Ag but Mg is missing these altogether and we expected Mg would have a greater effect on the s-d interactions in the alloy. Surprisingly, this was not found to be the case.

The apparatus used and the theory of the PRFE have been discussed previously[1,2,5] but will be included briefly in Sec. II for completeness and to clarify some minor points. Production and analysis of samples will be discussed in detail in Sec. III. Experimental results will be given in Sec. IV and discussed in Sec. V in comparison with Hall measurements, model calculations, and in terms of the scattering of the alloy conduction states. The results of other methods of measuring the Fermi surface of alloys will be discussed in Sec. VI and the conclusions of this work will be summarized in Sec. VII.

II. EXPERIMENTAL APPARATUS AND THEORY OF THE PRFE

The apparatus used for the PRFE measurements is shown in Fig. 1. It is essentially the same as that described in Refs. 1 and 2, except that the photomultipliers have been replaced by high-sensitivity silicon photovoltaic detectors. Also for some of the measurements, a special low-noise preamplifier was used. The end mirrors which take the beam into and out of the sample box were always evaporated gold films for the present work and the same end-mirror films were used for all measurements to avoid the possibility of relative errors caused by films of slightly different optical properties. The rotation and phase shift contributed by the end windows is compensated.

The response of a metal to incident electromag-

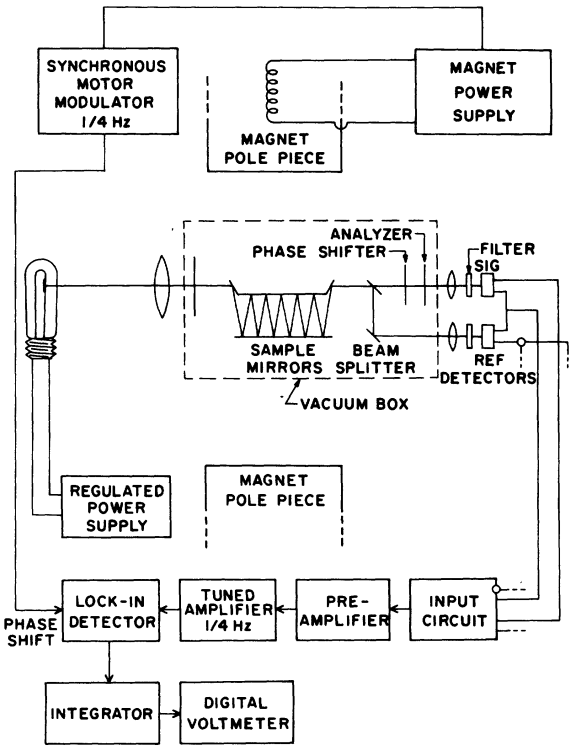

FIG. 1. Schematic drawing of the PRFE apparatus.

netic field $\vec{E}$, well above the cyclotron frequency, in the presence of a magnetic field $\vec{H}$, is given by

$$J_i = \sigma_{ij} E_j + \sigma_{ijk} E_j H_k + \cdots , \tag{1}$$

where H_k is the applied magnetic field and E_j is the electric field of the incident radiation. To first order in H and E and for a cubic metal with $\vec{H} = |H|\hat{z}$, one can write[5]

$$J_i = \sigma_{ij} E_j , \tag{2}$$

where

$$\sigma_{ij} = \begin{pmatrix} \tilde{\sigma}_0 & \tilde{\sigma}_1 & 0 \\ -\tilde{\sigma}_1 & \tilde{\sigma}_0 & 0 \\ 0 & 0 & \tilde{\sigma}_0 \end{pmatrix} . \tag{3}$$

The off-diagonal elements $\tilde{\sigma}_1$ are proportional to H and the real and imaginary parts of $\tilde{\sigma}_0$ are related to the ordinary optical constants. From Maxwell's equations, it can be shown that for normal incidence along the z direction, the Faraday rotation χ_s for initially s-polarized light (polarized out of the plane of incidence) of angular frequency ω is given by

$$\chi_s = \mathrm{Re}\, \frac{(-4\pi i/\omega)\hat{\sigma}_1}{(\hat{\epsilon}_0 - 1)[\sin^2\theta/\cos\theta + (\hat{\epsilon}_0 - \sin^2\theta)^{1/2}]} , \tag{4}$$

where $\hat{\epsilon}_0$ is the complex ordinary dielectric constant and θ is the angle of incidence. Similarly, the Faraday ellipticity Q_s is given by

$$Q_s = \mathrm{Im}\, \frac{(-4\pi i/\omega)\hat{\sigma}_1}{(\hat{\epsilon}_0 - 1)[\sin^2\theta/\cos\theta + (\hat{\epsilon}_0 - \sin^2\theta)^{1/2}]} . \tag{5}$$

Application of the Boltzmann transport equation for a high-frequency driving field and at an energy far below interband transitions gives

$$\hat{\sigma}_1 = \frac{e^3 H I_{FS}}{4\pi^3 \hbar^4 c \omega^2} , \tag{6}$$

where

$$I_{FS} = \int_{FS} \left[\frac{\omega\tau(k)}{\omega\tau(k) + i}\right]^2 \times \left(\frac{dE}{dk_x}\frac{d^2E}{dk_y^2} - \frac{dE}{dk_y}\frac{d^2E}{dk_y\, dk_x}\right) dk_y\, dk_z , \tag{7}$$

and c is the velocity of light. This expression involves the electron lifetimes $\tau(k)$ which are expected to be highly anisotropic for noble-metal alloys.[6,7] For dilute AgCd, Alderson and Hurd[7] find the lifetimes on the neck to be only about 60% of those on the belly portion of the Fermi surface. However, if the condition $\omega\tau \gg 1$ is satisfied in Eq. (7) then I_{FS} becomes dependent only on the E-versus-k relations for the electron states. I_{FS} may be written in a form which emphasizes Fermi surface geometry[5]:

$$I_{FS} = \frac{\hbar^2}{6}\int_{FS} v^2\left(\frac{1}{\rho_1} + \frac{1}{\rho_2}\right) dS , \tag{8}$$

where v is the Fermi velocity and ρ_1 and ρ_2 are the principal radii of curvature at a point on the Fermi surface. If $\omega \to 0$ in Eq. (7), I_{FS}/ω^2 becomes identical to the integral that occurs in the Hall effect in cubic metals.[8] So the PRFE is the high-frequency analog of the Hall effect and is more directly related to the Fermi-surface geometry than is the Hall effect. Also it should be noted that away from interband transitions and for $\omega\tau \gg 1$, χ_s is frequency independent.

Equation (8) can be used to determine the relative contributions of different parts of the Fermi surface to I_{FS}. Since the necks on the Fermi surface of pure Ag have one radius of curvature that is negative and small, these necks give a negative contribution. Therefore, a growth of the necks on alloying tends to decrease I_{FS} and this should be reflected in the observed rotation. However, I_{FS} also depends on the magnitude of the Fermi velocity, and this is expected to change on alloying. It is useful to define another quantity R which depends only on Fermi surface geometry and Fermi velocity anisotropy (not magnitude):

$$R = \frac{36\pi^3 n I_{FS}}{\hbar^2 (\int \vec{v}\cdot d\vec{S}_F)^2} , \tag{9}$$

where n is the conduction-electron density. R has the value unity for a spherical Fermi surface. Examination of Eq. (4) for the case of near normal incidence radiation in the near infrared shows that one can write

$$R = \frac{(4\pi n m_0)^{1/2} c \chi_I}{H} , \tag{10}$$

where χ_I is the frequency independent long-wavelength limit of the rotation and m_0 is related to $\int \vec{v}\cdot d\vec{S}_F$ by

$$m_0 = \frac{3(2\pi)^3 n\hbar}{2\int \vec{v}\cdot d\vec{S}_F} = \frac{-4\pi n e^2}{\omega^2(\epsilon_1 - 1)} . \tag{11}$$

Here ϵ_1 is the real part of $\hat{\epsilon}_0$ at the same long wavelength. This last form for R allows a combination of Faraday rotation and ordinary optical constant data to be used, in conjunction with model calculations, to obtain information on the change in neck diameter in concentrated alloys.

All the previous discussion depended on the condition $\omega\tau \gg 1$ and on the assumption that a Fermi surface can be defined for concentrated alloys. These assumptions can be tested by using the data for the Faraday ellipticity. Equations (4)–(7) show that Q and χ can be related to $\omega\tau$ by

$$\frac{Q}{\chi} = \frac{-2}{\omega\tau[1 - 1/(\omega\tau)^2]} . \tag{12}$$

For $\omega\tau$ small, this reduces to

$$Q/\chi = -2/\omega\tau \ . \qquad (13)$$

Then the condition $\omega\tau \gg 1$ becomes $|Q/\chi| \ll 2$. In addition, it is possible to obtain a rough estimate of the average smearing of the Fermi surface from the average τ obtained using Eq. (13).

III. SAMPLE PRODUCTION AND ANALYSIS

Samples were produced as opaque films on polished glass substrates in an evaporator described in detail by Erskine, Tracy, and Stern.[9] Briefly, an electron beam used as a heat source was electrostatically deflected between separate pellets of the alloy constituents. Each pellet was contained in a refractory-metal cup resting on a water-cooled copper hearth. The rate of evaporation of each constituent was monitored separately by quartz-crystal thickness monitors and the duty cycle of the electron beam on the two evaporants was controlled electronically so that the ratio of the masses of the two evaporants on the substrate was maintained at a preset value. This method of simultaneous evaporation eliminated the need for heating the sample to homogenize it and should reduce metallurgical problems, such as clustering, to a minimum. During the evaporation, the substrates were maintained at about 120°C to obtain reasonable crystallite size. At this temperature, movement of the atoms should be relatively easy on the surface as they hit but bulk diffusion should be small. Evaporations were carried out at pressures of 10^{-6} to 10^{-7} Torr.

X-ray diffraction determination of the lattice constant was used to determine concentration and verify the structure. The (111) peak for the alloys was the only useful peak that could be obtained so it was necessary to compare its position with the position of the (111) peak of a pure-Ag sample of identical geometry. This method eliminated errors due to sample geometry and absorption, and reduced errors due to thermal expansion of the lattice. A linewidth correction was applied to obtain true $K\alpha_1$ peak position, assuming Lorentzian line shape. Deviations from the assumed line shape caused by strains and constitutional inhomogeneities could contribute errors to the concentration determination but such errors are unlikely to exceed the uncertainties quoted. Figure 2 shows the diffractometer trace of a pure-Ag and an alloy (111) peak. The alloy linewidth decreased as the substrate temperature during evaporation increased from room temperature to 120°C. Heating of the substrates past 120 °C produced no further reduction of the linewidth.

Concentration gradients through the thickness of the sample are unlikely, owing to the method of sample production. However, it was found that

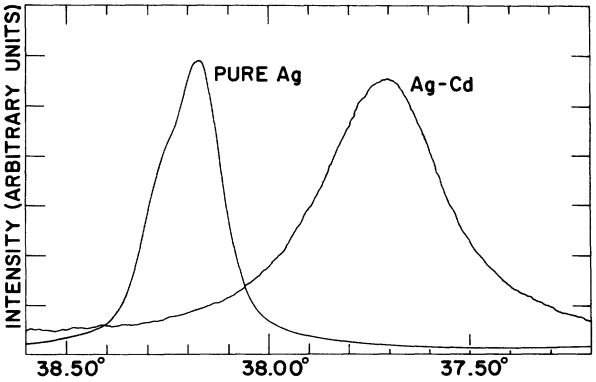

FIG. 2. Typical x-ray diffractometer traces for the (111) peaks in a pure-Ag and a AgCd sample.

concentration gradients along the sample slides amounted to several atomic percent impurity content in several cases, so the error bars on the data points represent the error in determining the average composition. The PRFE apparatus tended to sample the center portion of the slides, so the effect of the gradients was not significant compared to the errors in the measurement of the PRFE itself. In most cases, the errors were estimated to be ± 0.5 at.% impurity content. Any sample near the phase boundary that showed a trace of β phase was rejected. All samples were more than 1000 Å thick.

Prolonged exposure to clean air did not change the measured rotation. This was also found to be the case in Ref. 1 for pure Ag, Au, and Al samples. Unless irreversible surface contamination occurred during the first few minutes of exposure to air, this is evidence that the properties of the bulk metal has been measured.

The question of whether or not short-range order occurs in the alloys is an important one to consider. Measurements of the thermoelectric power by Henry and Schroeder[10] in bulk CuZn samples between 20- and 30-at.% Zn show strikingly different results depending on the annealing treatment and hence on the degree of short-range order. On the other hand, Auerback *et al.*[11] show very little dependence in the thermopower on the preparation in AgCd alloys. Since the thermopower is sensitive to short-range order, it is reasonable to assume that there is less short-range order in AgCd than in CuZn, and that the former alloy is more characteristic of a substitutionally completely disordered α-phase alloy. CuZn is known to have a low-temperature ordered phase around 25-at.% Zn. Waldman and Bever[12] have measured the resistivity of bulk AgCd samples as a function of annealing temperature and find that for slow cooling the degree of short-range order is equivalent to the equi-

librium value at about 450 °K. Since the present samples were evaporated onto substrates held at about 400 °K they should have a similar degree of short-range order, and it is reasonable to assume that the conclusions based on the thermopower measurements above also apply to the samples used for this work.

On the other hand AgMg has a much greater tendency toward long-range order than AgCd. An ordered α phase at 25 at.% Mg is known to occur. One would therefore expect that the AgMg alloys used in this study would have greater short-range order than the AgCd alloys. How this difference in short-range order effects the Fermi-surface changes would be of interest to note.

IV. EXPERIMENTAL RESULTS

Typical curves of the measured PRFE as a function of wavelength are shown in Fig. 3 for AgMg and AgCd. The wavelength dependence is small, similar to pure Ag, and it was straightforward to determine the long-wavelength limit χ_l. The curves show the data with various phase shifts added as described in Ref. 1. From these phase-shift data it is possible to separately determine χ and Q.

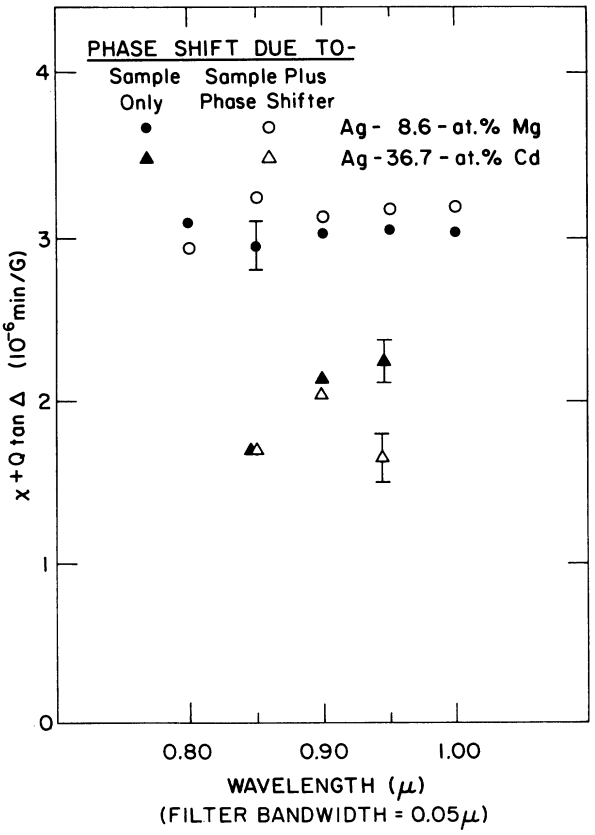

FIG. 3. Typical measured PRFE rotations vs wavelength for AgCd and AgMg and different phase shifts.

The measured long-wavelength limit of the Faraday rotation as a function of electron-per-atom ratio z obtained in this fashion is shown in Fig. 4. The line was drawn by eye and does not represent a calculated fit. The rotation for AgMg falls with increasing concentration of Mg up to about 30 at.% Mg, beyond which no α-phase samples could be produced. Up to about 30 at.% impurity, the rotation for AgCd follows closely that for AgMg, then falls more rapidly at higher Cd content.

Figure 5 shows the measured values for $-Q/\chi$, the ratio of Faraday ellipticity to rotation. There is a small rise toward higher concentrations as expected but the ratio is generally below 0.1. There are two fewer points in Fig. 5 than in Fig. 4 because two samples had anomalously high $-Q/\chi$ ratios. This was conclusively shown to be due to misalignment of the PRFE apparatus optics. It can be shown, however, that such misalignment should not affect the value of χ to within the errors shown and the χ data on these samples is retained. The other relatively high values of $-Q/\chi$ may also be due to the same effect although this is not certain.

If the typical value of $-Q/\chi$ is taken to be 0.1, then the corresponding mean lifetime from Eq. (13) is 1×10^{-14} sec, and the average smearing in the Fermi energy from the uncertainty principle is 0.06 eV.

V. DISCUSSION

In order to interpret the data in the light of Sec. II, it is necessary to show that the Fermi surface is reasonably well defined in the alloys. The conduction band in Ag is about 5 eV wide, so an uncertainty of 0.06 eV amounts to 0.01 fractional uncertainty. If the lifetime on the neck τ_N is about 60% that on the belly,[6] τ_B, then the fractional uncertainty in the vicinity of the neck becomes 0.02. This can be related to the uncertainty of the Fermi wave vector. If the E-versus-k relations were everywhere quadratic, the uncertainty in the wave vector would be less than 1%. However, near the necks, the velocity is decreased and the wave vector smearing is correspondingly increased. Taking this into account, the smearing of the Fermi surface is at most ten percent near the zone boundaries and considerably less elsewhere. Therefore the Fermi surface is reasonably well defined. More importantly, the changes in the Fermi surface for concentrated alloys are on the order of its dimensions. This means that the smearing is small compared to the changes and it is therefore possible to analyze these changes in terms of a sharp geometric surface. Whatever smearing is present will obscure fine details, particularly near critical points if there are any, but the behavior

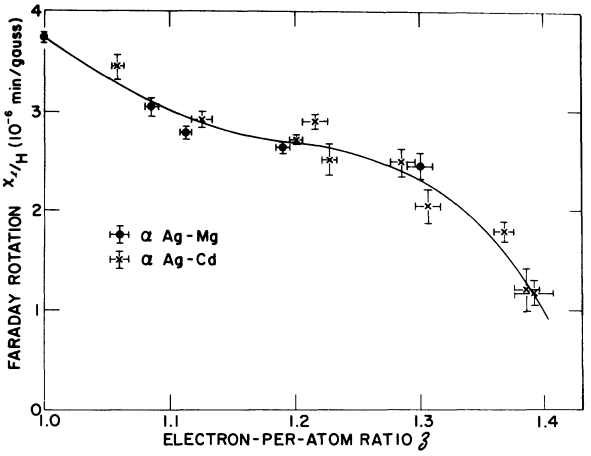

FIG. 4. The long-wavelength limit of the Faraday rotation as a function of electron-per-atom ratio for AgMg and AgCd.

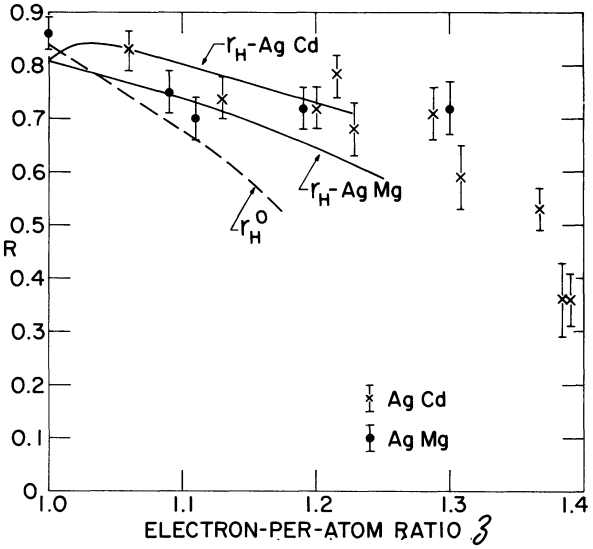

FIG. 6. The measured dimensionless parameter R (defined in the text) as a function of the electron-per-atom ratio $\mathfrak{z}$, indicated by the points. Plotted as the solid curves are r_H, ratios of the measured room-temperature Hall effect (Ref. 14) divided by the free-electron value at the density of electrons corresponding to $\mathfrak{z}$. The experimental errors associated with r_H are not given in the original reference (Ref. 14) and therefore are not shown in the curves. Also plotted is r_H^0, the ratio of measured Hall effect phenomenologically processed to supposedly eliminate the scattering anisotropy contribution (Refs. 16 and 17), divided by the free-electron value again. The disagreement between the experimental values of R and r_H^0 shows that the scattering anisotropy has not been eliminated.

on either side of the critical point should be determined by the average shape of the Fermi surface.

Equation (10) may be used to calculate the value of the dimensionless parameter R from χ_I/H, the electron density n, and the effective optical mass m_0, defined in Eq. (11). The values of m_0 are from Flaten and Stern[13] from optical-constant measurements made on samples produced in the same evaporator and by the same methods used in this work. In these measurements it is found that $\omega_p^2 = 4\pi ne^2/m_0$ is, to a good approximation, a constant, so that $m_0 \propto n$, the number of electrons per unit volume. The electron density was calculated by multiplying the density of electrons in pure silver by the $\mathfrak{z}$ (electron-per-atom ratio) of the alloys and by a small volume correction, since both impurities cause volume changes. The result is presented in Fig. 6 as a plot of R versus $\mathfrak{z}$.

In order to relate R to Fermi surface geometry, it is necessary to make some kind of model to compare with the measurements. This has been done in Ref. 1 for the analysis of Ag and Au. The model Fermi surface consists of a spherical belly and a neck section made up of a cylinder and a toroidal connecting piece. Velocities were selected in two different ways: constant velocity over the entire surface in one case and a varying ratio of neck to belly velocities in the other. Figure 7 shows the results of the calculation. The neck radius r_n is given in terms of the radius of the free-electron sphere r_0 that contains the same number of electrons per atom. The four curves represent four cases as follows: (a) The neck consists entirely of the toroidal joint section (no cylinder) and the velocity is a constant over the entire surface. (b) The neck consists entirely of the cylinder (no toroidal section) and the velocity is a constant. (c) Similar to case (a) but the velocity is constant over the belly and has a different value over the joint section. (d) Similar to case (b) but with different values over the belly and cylinder section. Cases (c) and (d) have more physical velocity distributions and case (c) has a more

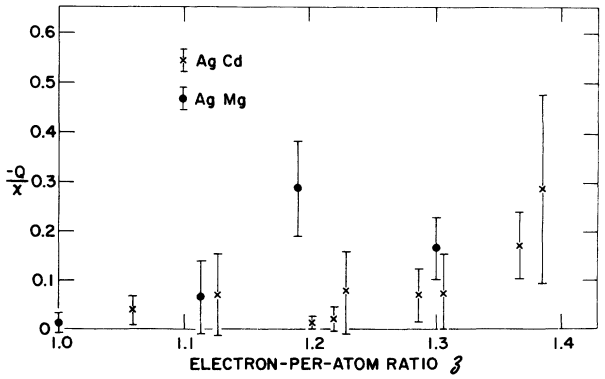

FIG. 5. The ratio of Faraday ellipticity to rotation as a function of electron-per-atom ratio for AgMg and AgCd.

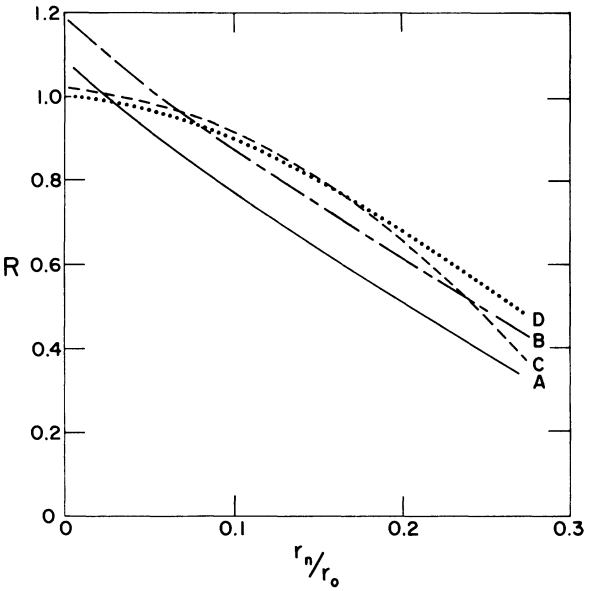

FIG. 7. Dimensionless parameter R as a function of the ratio of the Fermi-surface neck radius r_n to the free-electron sphere radius r_0, in four different models for Ag. See text for explanation of curves A through D.

realistic neck profile.

The actual velocity anisotropy over the Fermi surface, the neck shape, and the variation of both with concentration are unknown in the alloys. However, the range of assumptions covered by curves A to D should include any reasonable possibility for these variations and we see the general trend of R decreasing as r_n/r_0 increases. The variation in r_n/r_0 between the curves for a given R preclude any accurate determination of r_n/r_0 from the model without additional information on the velocity anisotropy. However, the measured decrease in R shown in Fig. 6 clearly indicates that the necks on the Fermi surface are increasing with concentration at a faster rate than the radius r_0 of the free-electron sphere which contains the same $\mathfrak{z}$, and thus faster than r_B, an average belly radius which will be smaller than r_0.

Figure 6 also clearly indicates that the variations in the Fermi surface of both AgMg and AgCd are the same as a function of $\mathfrak{z}$ within experimental error over their common range. At first thought this result is surprising. The large gap in the noble metals is attributed to the s-d hybridization. Any change in the d levels on alloying would affect this gap and thus the size of the neck. Cadmium has d levels several electron volts below that of Ag, while Mg has its d levels many electron volts above that of Ag. Off-hand one would expect that Mg and Cd would therefore affect the d levels of the alloys in differing amounts. If this were so the neck growth with alloying would reflect this by a different variation between AgCd and AgMg. One is forced to conclude that the d levels in AgCd and AgMg vary in the same way. Recent direct measurements of the position of the top part of the d bands in AgCd and AgMg were made by investigating their optical constants.[13] These results confirm that the d band in AgCd and AgMg behave similarly with alloying in agreement with the results of this paper. Another conclusion to be drawn from the similar Fermi surface for AgMg and AgCd is that the Fermi surface does not depend strongly on short-range order. As pointed out at the end of Sec. III, AgMg is expected to have more short-range order than AgCd.

Also plotted on Fig. 6 are r_H, the ratios of the room-temperature Hall effect in the alloys[14] to the value R_f expected for a free-electron sphere enclosing the same $\mathfrak{z}$. The value R_f is inversely proportional to n, the number of electrons per unit volume. Thus an account was taken of the volume changes on alloying as was done in determining R. The errors in the Hall-effect measurements are not given in Ref. 14, but from the behavior of the data for AgCd and AgMg it is not unreasonable to assume error bars similar to those for R. By referring to Eqs. (7) and (9) and the intervening discussion, we note that $r_H = R$ if τ is a constant independent of $\vec{k}$ on the Fermi surface. By this same type of reasoning,[15] $r_H < R$ if $\tau_N > \tau_B$, where τ_N is an average lifetime on the neck, which gives a negative contribution to R, and τ_B is an average lifetime on the rest of the belly part of the Fermi surface which contributes positively to R. Conversely, $r_H > R$ if $\tau_N < \tau_B$. Within experimental error $\tau_N = \tau_B$ for both AgCd and AgMg. Including error estimates we obtain $\tau_N/\tau_B = 1 \pm 0.2$ for the concentrated range at room temperature, as compared to 0.6 for dilute alloys.[6]

The final curve plotted in Fig. 6, labeled by r_H^0, is the result of attempts by Hurd[16] and Barnard[17] to separate out the scattering anisotropy effects in r_H and obtain R from Hall-effect measurements for Ag-based alloys. The reasoning used by these authors will not be discussed here. Reference to the original articles can be made to discover these details but it is clear that their assumptions are incorrect: r_H^0 deviates significantly from R. This illustrates conclusively that Hall-effect measurements by themselves are not sufficient to determine separately the shape variations and the scattering anisotropy over the Fermi surface. Hall-effect measurements depend on both these effects and some other measurement such as the PRFE is necessary to separate the two.

From the values of R plotted in Fig. 6 and the model calculation of Fig. 7 it is possible to plot the experimental data as r_n/r_0 versus $\mathfrak{z}$. However, as indicated before, there is not enough ex-

perimental data to specify all parameters of the model calculation. In particular, the velocity anisotropy over the Fermi surface is unknown. The curve C in Fig. 7 is the most physically realistic of the ones shown and it assumes that at $r_n/r_0 = 0.3$, the average velocity squared on the neck equals that on the belly. This is a somewhat arbitrary assumption and one could argue just as well that this equality could occur at $r_n/r_0 = 0.4$. The difference in this assumption does not influence the results of Ref. 1 appreciably but it does significantly influence the values of r_n/r_0 for larger $\mathfrak{z}$. We have added this calculational uncertainty to the experimental uncertainties in the plotted points in Fig. 8.

For comparison we plot in Fig. 8 the initial slope in r_n/r_0 calculated for the rigid-band model. This is obtained from experimental data as summarized in Ref. 18. To within 1% the electronic specific heat of Ag equals that of a free-electron gas. Thus in the rigid-band model the variation of r_0 with the number of electrons per unit volume n can be approximated by a free-electron gas. The measured velocity[18] on the Ag neck is $0.35v_0$, where v_0 is the free-electron Fermi velocity. For a given change in energy ΔE, the ratio $\Delta r_n/\Delta r_0$ is equal to $(0.35)^{-1}$. By this means the initial slope $d(r_n/r_0)/d\mathfrak{z}$ was calculated and plotted in Fig. 8. The small difference in slope between AgMg and AgCd arises from their different expansion on alloying. We note that within experimental error the measured initial slope agrees with the rigid-band model.

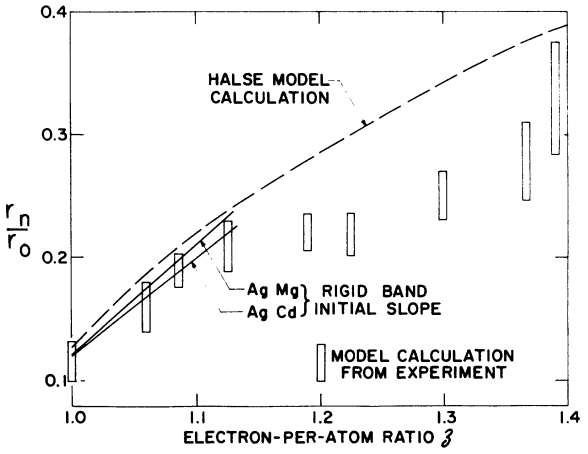

FIG. 8. The bars are the ratio of the neck radius r_n to the radius of the free-electron Fermi-surface sphere r_0, as determined by the experiment based on the model of Fig. 7. Some of the bars are averages over several experimental points. For comparison, a model of Halse is used for a rigid-band-model calculation shown as the dashed curve. The rigid-band initial slopes for AgCd and AgMg as determined from experimental data are also shown.

The dashed curve in Fig. 8 was obtained from a rigid-band-model calculation done for the present work. The simplest rigid-band model assumes that the E-versus-k curves for the pure metal are unchanged in the alloy and the Fermi surface simply expands to accommodate the extra electrons. Thus the constant-energy surfaces of the pure metal define the shape of the Fermi surface in the alloy. This model is not realistic since the energies of the states must change as alloying occurs but it serves as a useful starting point for the analysis. What is needed is a set of surfaces having the symmetry appropriate for the fcc lattice and having the shape of the Fermi surface of pure Ag when one electron per atom is enclosed. Since there are no measurements of the constant energy surfaces above the Fermi energy, it is necessary to approximate these from data taken on pure Ag. To this end, the expansion of Halse[18] has been used to generate surfaces that meet the above criterion. The Fermi surface of Ag was obtained by fitting a five-term Fourier expansion to de Haas–van Alphen data on Ag. The expansion parameters used in this work are the set Ag5 in Halse's notation. It should be pointed out that the expansion parameters are appropriate only for the Fermi surface of Ag and are not meant to describe other constant-energy surfaces rigorously. In fact, Halse uses an entirely different set of parameters to describe surfaces just above and below the Fermi surface to obtain velocity values. However, if only his parameter C_0 is varied, the dashed curve in Fig. 8 results with an initial slope not too different from the rigid-band estimates. It is therefore not unreasonable to hope that the results are reasonably accurate for all $\mathfrak{z}$. The electron-per-atom ratio is obtained for each C_0 by calculating the volume of the surface. Quantities which depend only on Fermi-surface geometry may be calculated and relative values of other quantities can be obtained by computing surfaces just above and below the chosen surface. Since C_0, not energy, is the expansion parameter, quantities that involve the derivatives of energy will require the knowledge of the derivative of C_0 with respect to energy. This can be obtained from band structure calculations. It is found that C_0 varies fairly linearly with energy, so unless absolute values are needed, a plot of relative values, which can be obtained, will suffice. This will be discussed further later.

Figure 9 shows cross sections of the surfaces generated. Note the increase in the radius of the primary set of necks and the occurrence of a second set of necks at X which occurs for electron-per-atom ratios greater than 1.33. The semicircles are cross sections of free-electron spheres for $\mathfrak{z} = 1.00$ and 1.33. Larger values of C_0 produce larger surfaces. The primary neck radius is

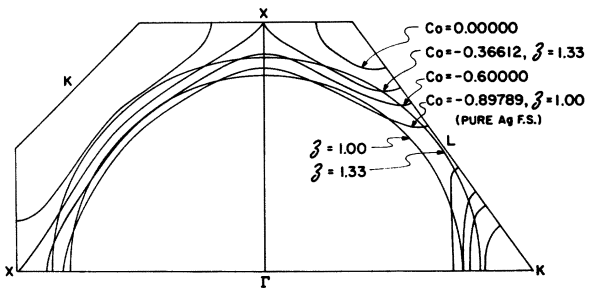

FIG. 9. Cross sections of the surfaces generated using Halse's expansion parameters. The hemispheres are cross sections of spheres containing 1.00 and 1.33 electrons per atom.

plotted against ϑ in Fig. 8. The first conclusion that can be drawn from Fig. 8 is that although initially the necks grow at the rigid-band rate, they grow more slowly than the rigid-band-model rate for higher concentrations, except right near the phase boundary at $\vartheta = 1.4$.

Near $\vartheta = 1.4$ the data could be interpreted as an increase in the rate of growth of r_n/r_0. Another possible interpretation to this increased rate of growth is the occurrence of second contact. The plot in Fig. 8 assumed that only contact along the [111] direction occurs in calculating r_n/r_0. If a second contact occurs this would add a new rate of decrease of R to that contributed by the first contact, which could explain the increase of r_n/r_0 near $\vartheta = 1.4$. Unfortunately the present experimental data are not accurate enough to justify any definite statement concerning second contact, but it is suggestive that second contact may be occurring near $\vartheta = 1.4$.

Since the neck sizes are smaller for the real alloys than for the rigid-band model in the concentrated regime, the alloy surface is somewhat more spherical than in the rigid-band model. It is then reasonable to expect that if a second set of necks is produced, this would occur at larger ϑ ratios than in the model calculation. This means that if the necks occur at all they do so very near the α-phase boundary, consistent with the suggestion of the data. This has a bearing on the discussion of the Hume-Rothery rules to be taken up later. The fact that the primary necks initially grow at a rate about that predicted by the rigid-band model is consistent with de Haas–van Alphen measurements[19] on dilute Ag- and Cu-based alloys.

The slower growth of the primary neck can be understood if the energy gap at the Brillouin zone decreases on alloying. Then the distortion of the Fermi surface would be less than in the rigid-band model, where the energy gap is assumed to remain constant. The gap would decrease if the d levels lower on alloying and decrease the s-d hybridization. Optical measurements[13] show such a lowering, consistent with our result here.

Considerable work has been devoted to the understanding of the Hume-Rothery rules. The simplest theories attributed the phase transition to the sudden change in the rate of variation of the free energy of a structure when the Fermi surface touched the Brillouin-zone boundary. After it was discovered that the Fermi surface in the noble metals touch even for no impurity content, Hume-Rothery and Roaf[20] proposed that the phase transformation occurs just after second contact. Figure 10 shows their estimate of the density of states in pure Ag for the case where second contact occurs. The Fermi energy of pure Ag lies just to the right of the first low-energy peak. The validity of their theory depends on the relative size of the second peak, which is taken to be substantial. A better estimate of the peak height may be obtained with the rigid-band model discussed earlier in this paper. The density of states calculated with this model is shown in Fig. 11. This curve is quite different from that of Hume-Rothery and Roaf. The second peak is at most 2% of the total density of states and it seems unlikely the change in the free energy due to this peak could cause the phase transition.

Our experiment definitely proves that the whole class of explanations of the Hume-Rothery rules which depend on the properties of the Fermi surface of only the α phase is inadequate. Both AgCd and AgMg have the same Fermi surface in the concentration region where they overlap, yet AgCd is a Hume-Rothery alloy while AgMg is not. Thus the second-contact explanation is inadequate on the basis of our experiment alone, although it is satisfying that the rigid-band calculation illustrated in Fig. 11 confirms this. To understand the difference between AgCd and AgMg, one must refer to the second phase to which each transform. The

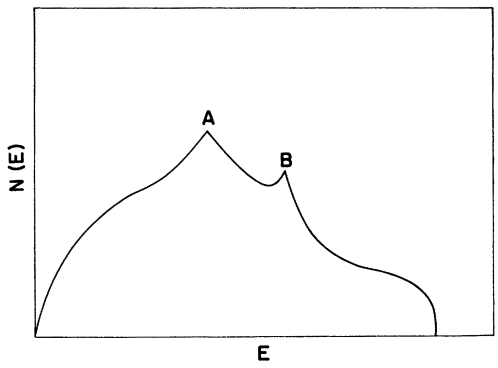

FIG. 10. Qualitative density of states for Ag assuming second contact occurs, from Hume-Rothery and Roaf (Ref. 20).

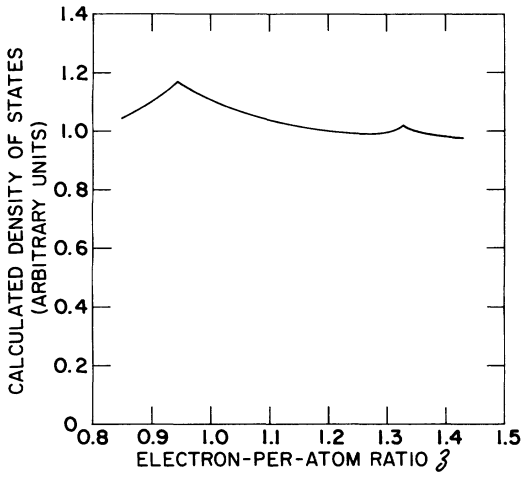

FIG. 11. Density of states calculated from the rigid-band model discussed in the text.

second phase for AgMg is an ordered β' phase with lower energy than the disordered β phase. This greater stability of the β' phase presumably is a large factor in causing the α phase of AgMg to transform at a lower $\bar{z}$ than does AgCd.

Stroud and Ashcroft[21] propose a new mechanism to account for the phase transformation. They attribute the change in the energy of a structure to the change in the characteristic of the dielectric function whenever the Fermi surface touches the Brillouin-zone boundary. This results in the same predictions as for the earlier theories in that the anomaly in the dielectric screening function occurs at the same $\bar{z}$ ratio as the peak in the density of states due to zone contact. As pointed out, both phases must be considered when determining relative phase stability. In fact, Stroud and Ashcroft attribute the position of the α-phase boundary in CuZn to zone-boundary touching in the β-phase structure. Heine and Weaire[22] criticize this screening argument and state that details of the Fermi surface are not important to the stability of the α and β phases in noble-metal alloys. They believe, and so do we, that any calculation of phase stability is incorrect unless the d bands are considered. Stroud and Ashcroft ignore the effects of the d bands. However, optical measurements[13] indicate the same d-band behavior for AgMg and AgCd, making it clear that their different behavior with respect to the Hume-Rothery rules comes from the differences in their second phase.

VI. DISCUSSION OF OTHER EXPERIMENTS

There are other experiments which yield information about the Fermi surface of concentrated alloys. A few of these will be discussed to the extent that they bear on the conclusions presented here.

The de Haas–van Alphen work of Coleridge[19] has already been discussed. Chollet and Templeton[23] have made de Haas–van Alphen measurements on dilute Cu-based alloys. They find good agreement in CuZn alloys between observed neck variations and rigid-band expectations. Their measurement of neck scattering temperature is roughly 24 °K/at.% Zn for a 0.1-at.% alloy. Extrapolated to 40% impurity, this yields an uncertainty of 0.08 eV for the Fermi energy in the vicinity of the neck. This agrees to within a factor of 2 with the estimate made earlier in the present work for AgCd. There have been no de Haas–van Alphen measurements to date in AgCd.

Measurement of the residual resistivity should also give an estimate of the smearing of the energy. Seth[24] obtains a value of 0.4761 $\mu\Omega$ cm for a Ag–1.43-at.% Cd alloy. Using a simple free-electron relaxation-time model, this value of the resistivity gives an average uncertainty in the energy of 0.005 or 0.15 eV for a 42-at.% alloy. The resistivity at high concentrations should be smaller than the linearly extrapolated value, so 0.15 eV is an overestimate of the smearing and this result is in good agreement with the PRFE measurements.

Two experimental quantities give direct measures of the density of states—specific heat and magnetic susceptibility. The former experiment has been carried out on AgCd by Montgomery *et al.*,[25] while other Ag-based alloys have been studied by others.[26,27] All results show an increase in the electronic specific heat as the $\bar{z}$ ratio is increased. This is in apparent contradiction to the rigid-band model which shows a decreasing density of states. However, Stern[28] has shown that specific-heat measurements cannot be interpreted in terms of the rigid-band model but should be interpreted in terms of the charge buildup due to shielding of impurities. Ideally, any structure in the density of states, such as the peak in Fig. 11, should still show up in the specific-heat data. However, the data have sufficient error and the peak in the density of states is so small that it may be missed even if it is present. It should be noted that there is an unexplained peak in the data[26] for CuZn at around 10-at.% Zn. It is quite possible that this is due to short-range order known[11] to occur in CuZn and does not reflect a critical point in the density of states.

Magnetic susceptibility should naively be related to the density of states in the same way as specific heat. However, uncertainties in the core-diamagnetism correction preclude definite statements about the electronic density of states at this time.

Positron annihilation experiments have been carried out in noble metals only on Cu-based alloys.[29–32] These show that the neck diameter has increased on alloying but there is no evidence of

second touching. These experiments are difficult to carry out and to analyze and there are large discrepancies between the results of different workers on the same alloy. It is unlikely that useful experiments on Ag-based alloys will be made in the near future since the positron source must be external to the sample and fewer counts can be obtained.

VII. CONCLUSIONS

The main conclusions of this work are that the Fermi surfaces of concentrated AgMg and AgCd α-phase alloys are well defined and that there is a growth of the necks on the Fermi surface as the impurity concentration is increased. The uncertainty in energy of states on the neck part of the Fermi surface is on the order of 1% of the conduction bandwidth. The change in the neck diameter due to alloying may be estimated from a simple model and compared to the change expected in a rigid-band model. For the models chosen, the initial experimental neck size increase is consistent with the rigid-band model but for intermediate concentrations grows less rapidly than for the rigid-band model. One explanation of this is that the energy gap is reduced due to the reduction of s-d hybridization as Ag atoms are replaced by impurity atoms. The Fermi surfaces of the α-phase of both AgCd and AgMg have the same variation in shape within experimental error in the overlapping concentration region where they are both stable. The scattering relaxation time on the necks is the same as on the belly within about 20% for both AgMg and AgCd. From this equality of Fermi-surface properties for AgMg and AgCd, and the equality in their d-band behavior implied by this Fermi-surface equality and confirmed by optical measurements, we conclude that any explanation of the Hume-Rothery rules must include the second phases. AgMg is not an Hume-Rothery alloy while AgCd is. The present PRFE data are not sufficiently precise to confirm second contact for AgCd, but the data suggest that this may occur near an electron-per-atom ratio $\frac{e}{a}$ of 1.4. AgMg is not stable to a high enough $\frac{e}{a}$ for a second contact to occur. The rigid-band calculation suggests that second touching would not have important consequences for electronic properties even if it does occur.

With the possible exception of positron annihilation, the polar reflection Faraday effect can yield the best information on Fermi-surface shapes of concentrated (greater than 1-at.% impurity) noble-metal alloys of all experimental methods attempted so far.

---

*Research sponsored in part by the National Science Foundation, Grant No. GU-2655, Science Development Grant, and in part by the Air Force Office of Scientific Research, Office of Aerospace Research, USAF, under Grant No. AFOSR 71-1967. The United States Government is authorized to reproduce and distribute reprints for governmental purposes notwithstanding any compyright notation hereon.

†Present address: Physics Department, Michigan State University, East Lansing, Mich. 48823.

[1]J. C. McGroddy, A. J. McAlister, and E. A. Stern, Phys. Rev. **139**, A1844 (1965).

[2]A. J. McAlister, E. A. Stern, and J. C. McGroddy, Phys. Rev. **140**, A2105 (1965).

[3]E. A. Stern, Phys. Rev. **188**, 1163 (1969); Summer School on Alloys, Physics Dept., Michigan State University, E. Lansing, Mich., 1972; Phys. Rev. B **7**, 1303 (1973).

[4]N. F. Mott and H. Jones, *The Theory of the Properties of Metals and Alloys* (Dover, New York, 1958).

[5]E. A. Stern, J. C. McGroddy, and W. E. Harte, Phys. Rev. **135**, A1306 (1964).

[6]This result is found for some dilute noble-metal alloys (no measurements were done on AgCd and AgMg) by D. H. Lowndes, K. Miller, and M. Springford, [Phys. Rev. Lett. **25**, 1111 (1970)]. The analysis to be given below estimates that $\tau_N \simeq \tau_B$. In addition, the τ determined in PRFE is the transport τ which, because of the $(1 - \cos\theta)$ factor, is about a factor of 2 less than both the τ measured in de Haas–van Alphen effect and the one that determines the uncertainty in the Fermi surface. These distinctions will not be made in our discussion, since they are within the accepted uncertainties of our estimates.

[7]J. E. A. Alderson and C. M. Hurd, Can. J. Phys. (to be published).

[8]M. Tsuyi, J. Phys. Soc. Jap. **13**, 979 (1958).

[9]J. L. Erskine, J. M. Tracy, and E. A. Stern, Rev. Sci. Instrum. **42**, 501 (1971).

[10]W. Henry and P. A. Schroeder, Can. J. Phys. **41**, 1076 (1963).

[11]H. Auerbach, D. Flynn, S. Goetsch, C. C. Lee, and P. A. Schroeder (unpublished).

[12]J. Waldman and M. B. Bever, Can. J. Phys. **3**, 1607 (1972).

[13]C. Flaten and E. A. Stern (unpublished).

[14]W. Koster and H. P. Rave, Fiz. Met. Metalloved. **55**, 750 (1964).

[15]See also J. S. Dugdale and L. D. Firth, J. Phys. C **2**, 1272 (1969); Phys. Kondens. Mater. **9**, 54 (1969).

[16]C. M. Hurd, Philos. Mag. **14**, 647 (1966).

[17]R. D. Barnard, Philos. Mag. **14**, 1097 (1966).

[18]M. R. Halse, Philos. Trans. R. Soc. Lond. A **265**, 507 (1969).

[19]P. T. Coleridge (private communication); P. T. Coleridge and I. M. Templeton, Can. J. Phys. **49**, 2449 (1971).

[20]W. Hume-Rothery and D. J. Roaf, Philos. Mag. **6**, 55 (1961).

[21]D. Stroud and N. W. Ashcroft, J. Phys. F **1**, 113 (1971).

[22]V. Heine and D. Weaire, Solid State Phys. **24**, 249 (1970).

[23]L. F. Chollet and I. M. Templeton, Phys. Rev. **170**, 656 (1968).

[24]R. S. Seth, Phys. Rev. B **2**, 2961 (1970).

[25]H. Montgomery, G. P. Pells, and E. M. Wray, Proc. R. Soc. A **301**, 261 (1967).

[26]U. Mizutane, S. Noguchi, and T. B. Massalski, Phys. Rev. B **5**, 2057 (1972)

[27]B. A. Green, Jr. and H. V. Culbert, Phys. Rev. **137**, A1168 (1965).

[28]E. A. Stern, Phys. Rev. B **1**, 1518 (1970).

[29]K. Fukiwara, O. Sueoka, and T. Imura, J. Phys. Soc. Jap. **24**, 467 (1968).

[30]D. L. Williams, E. H. Becker, and P. Petyevich, Bull. Am.

Phys. Soc. **14**, 402 (1969).
[31]B. W. Murray and J. D. McGervey, Phys. Rev. Lett. **24**, 9 (1970).
[32]A. Thompson, B. W. Murray, and S. Berko, Phys. Lett. A **37**, 461 (1971).

PHYSICAL REVIEW B VOLUME 8, NUMBER 2 15 JULY 1973

Study of Phonon Dispersion in hcp Metals with Central Pair Potentials Representing Ion-Ion Interactions

J. C. Upadhyaya and M. P. Verma
Department of Physics, Agra College, Agra-2, India
(Received 18 September 1972)

A phenomenological model for the study of the lattice dynamics of hcp metals has been developed by adding an approximate electron-ion-interaction term to a five-neighbor central pair potential. Application of the model to the four hcp solids Mg, Sc, Zr, and Ho leads to dispersion curves which generally present a good agreement with the corresponding experimental curves.

I. INTRODUCTION

Dispersion curves of a large number of hcp metals have been determined in recent years by the neutron-spectroscopic method. These curves provide the basic information for an understanding of the dynamics of the hcp lattice. The models generally employed for theoretical explanations of these curves are tensor-force (TF) model, the axially symmetric (AS) model, the modified axially symmetric (MAS) model, and a mixed-force (MF) model based on axially symmetric interactions and tensor forces acting among various neighbors.[1-5] Such models employ a large number of parameters and agreement with experimental curves, achieved by means of a least-squares fitting procedure, is often excellent. However, the fact that these models do not incorporate the metallic character of the solids makes them unsatisfactory from the theoretical point of view.

A relatively recent work on the lattice dynamics of the hcp system is that presented by King and Cutler[6] and is based on a model pseudopotential calculation. This work must be considered theoretically satisfactory, but the results of this study also show large deviations from experimental dispersion curves.

A serious question concerning theoretical models of lattice dynamics has been recently raised by Szigeti and co-workers.[7,8] These authors have shown from general considerations that the parameters of a theoretical model can be continuously varied over large ranges without affecting the order of agreement between the theory and the experiment. It has been pointed out that a unique set of values of the model parameters can in principle be determined if we also possess additional results on measurements of eigenvectors or those obtained by substitution of isotopes. In view of this work, the agreement with dispersion data can not be considered as enough proof of the validity of a theoretical model. However, until measurements on eigenvectors are available, the dispersion data will continue to remain the most dependable experimental results for theoretical workers in the field of lattice dynamics. In order to decide upon the superiority of one theoretical model over another, we can appeal to the principle of simplicity and the plausibility of the basic assumptions.

The main points of deviation from the lattice dynamics of cubic metals in the case of the hcp system are (i) the lower symmetry of this system and (ii) the range to which the ion-ion interactions are significant. The TF and AS models satisfy the symmetry conditions but have to employ force constants out to eighth neighbors for the best agreement with experimental dispersion curves. In view of the screening effect of the conduction electrons, it seems unlikely that the ion-ion interactions are significant out to such distant neighbors. In the work presented here we have tried to investigate this point phenomenologically using a force model that includes the effect of conduction electrons along the lines used by Sharma and Joshi[9] for cubic metals. The resulting electron-ion interaction does not satisfy the requirements of symmetry in the reciprocal space but can be considered satisfactory as far as numerical results are concerned. The ion-ion interactions have been derived from pair potentials. Such a representation of the ion-ion interactions has been discussed by Lahteenkorva,[10] but to reduce the number of parameters of his theory, so that they could be evaluated mainly from the expressions for the five elastic constants, he has used additional constraints and set some of the potential parameters equal to zero, resulting